

# NAVAL POSTGRADUATE SCHOOL MONTEREY, CALIFORNIA



## THESIS

### FINITE DIFFERENCE METHODS APPLIED TO BIOT THEORY IN POROUS MEDIUM

by

Jonah Wai Shen

September, 1995

Thesis Advisor:

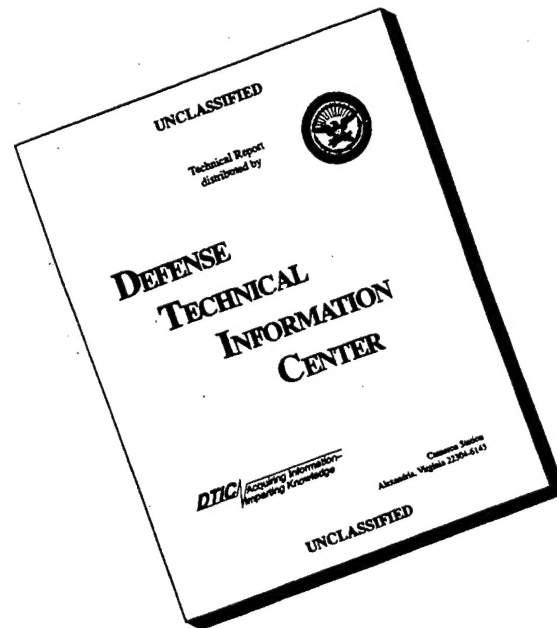
Clyde Scandrett

Approved for public release; distribution is unlimited.

19960402 147

DTIC QUALITY INSPECTED 1

# DISCLAIMER NOTICE



**THIS DOCUMENT IS BEST QUALITY AVAILABLE. THE COPY FURNISHED TO DTIC CONTAINED A SIGNIFICANT NUMBER OF PAGES WHICH DO NOT REPRODUCE LEGIBLY.**

REPORT DOCUMENTATION PAGE			Form Approved OMB No. 0704-0188	
Public reporting burden for this collection of information is estimated to average 1 hour per response, including the time for reviewing instruction, searching existing data sources, gathering and maintaining the data needed, and completing and reviewing the collection of information. Send comments regarding this burden estimate or any other aspect of this collection of information, including suggestions for reducing this burden, to Washington Headquarters Services, Directorate for Information Operations and Reports, 1215 Jefferson Davis Highway, Suite 1204, Arlington, VA 22202-4302, and to the Office of Management and Budget, Paperwork Reduction Project (0704-0188) Washington DC 20503.				
1. AGENCY USE ONLY (Leave blank)		2. REPORT DATE September 1995		3. REPORT TYPE AND DATES COVERED Master's Thesis
4. TITLE AND SUBTITLE FINITE DIFFERENCE METHODS APPLIED TO BIOT THEORY IN POROUS MEDIUM (U)			5. FUNDING NUMBERS	
6. AUTHOR(S) Shen, Jonah W.				
7. PERFORMING ORGANIZATION NAME(S) AND ADDRESS(ES) Naval Postgraduate School Monterey CA 93943-5000			8. PERFORMING ORGANIZATION REPORT NUMBER	
9. SPONSORING/MONITORING AGENCY NAME(S) AND ADDRESS(ES)			10. SPONSORING/MONITORING AGENCY REPORT NUMBER	
11. SUPPLEMENTARY NOTES The views expressed in this thesis are those of the author and do not reflect the official policy or position of the Department of Defense or the U.S. Government.				
12a. DISTRIBUTION/AVAILABILITY STATEMENT Approved for public release; distribution is unlimited.			12b. DISTRIBUTION CODE	
13. ABSTRACT (maximum 200 words) Finite difference methods are used to solve the Biot equations for wave propagation in a porous medium. The computational domain is a two dimensional grid of uniform spacing where truncation of the grid on all sides is accomplished by applying homogeneous Dirichlet boundary conditions. The difference method is second order in space and time, and is seen to accurately predict phase speeds of the primary compressional and shear waves.				
14. SUBJECT TERMS Finite Difference Methods Biot Theory Porous Medium			15. NUMBER OF PAGES 54	
			16. PRICE CODE	
17. SECURITY CLASSIFICATION OF REPORT Unclassified	18. SECURITY CLASSIFICATION OF THIS PAGE Unclassified	19. SECURITY CLASSIFICATION OF ABSTRACT Unclassified	20. LIMITATION OF ABSTRACT UL	



Approved for public release; distribution is unlimited.

**FINITE DIFFERENCE METHODS APPLIED TO BIOT  
THEORY IN POROUS MEDIUM**

Jonah W. Shen  
Lieutenant, United States Navy  
B.S., United States Naval Academy, 1987

Submitted in partial fulfillment  
of the requirements for the degree of

**MASTER OF SCIENCE IN ENGINEERING ACOUSTICS**

from the

**NAVAL POSTGRADUATE SCHOOL**

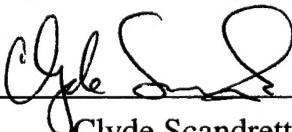
**September 1995**

Author:

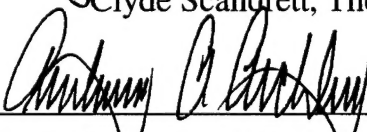


Jonah W. Shen

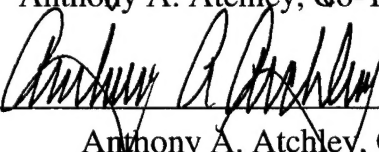
Approved by:



Clyde Scandrett, Thesis Advisor



Anthony A. Atchley, Co-Thesis Advisor



Anthony A. Atchley, Chairman  
Engineering Acoustics Academic Committee



## **ABSTRACT**

Finite difference methods are used to solve the Biot equations for wave propagation in a porous medium. The computational domain is a two dimensional grid of uniform spacing where truncation of the grid on all sides is accomplished by applying homogeneous Dirichlet boundary conditions. The difference method is second order in space and time, and is seen to accurately predict phase speeds of the primary compressional and shear waves.





## TABLE OF CONTENTS

I. INTRODUCTION.....	1
II. THEORY.....	3
A. WAVE EQUATIONS.....	3
B. BOUNDARY CONDITIONS.....	6
C. SOURCE FUNCTION.....	7
III. PROGRAM ALGORITHM.....	9
A. FINITE DIFFERENCE SCHEME.....	9
B. SCALING.....	17
C. STABILITY.....	18
D. PARAMETERS.....	19
E. DISCUSSION.....	21
IV. CONCLUSION.....	31
APPENDIX PROGRAM CODE.....	33
LIST OF REFERENCES.....	41
BIBLIOGRAPHY.....	43
INITIAL DISTRIBUTION LIST.....	45



## I. INTRODUCTION

Mine warfare has resurfaced as a major concern for the United States after the Gulf War. The *Tripoli* and the Aegis cruiser *Princeton* suffered mine strikes, driving home the danger of mines and the need for effective intelligence and mine countermeasures. In 1992, the Chief of Naval Operations reorganized the Navy headquarters establishing a Director, Expeditionary Warfare (N85). At this time, the Navy also established the Program Executive Office for Mine Warfare - reporting directly to the Assistant Secretary of the Navy for research, development, and acquisition. [Ref. 1]

The United Nations estimates that during recent civil and international strife, more than 100 million mines have been laid in 62 countries. A United States government report estimates that the worldwide total of deployed land mines increases by 500,000 to 1 million each year. After troops withdraw, land mines and unexploded ordnances remain in the ground, killing and maiming scores of people - farmers, travelers, workers, soldiers - every day indiscriminately. The Secretary general of the United Nations Boutros Boutros-Ghali now urges stronger political and financial support for efforts to neutralize mines worldwide. [Ref. 2]

In search of a better means for buried mine detection, BBN Systems and Technology completed a study experimenting with Rayleigh waves for mine detection in 1992. The results of their study claimed the probability of detection for anti-tank mines is from 74% to 80% and 17 % for anti-personnel mines . The maximum detection range reported was found to be 15 feet. [Ref. 3]

Currently, the Naval Postgraduate School is conducting experiments based on Rayleigh wave propagation as mentioned in the BBN report. The goal of the research is to improve detection range and the probability of detection of buried objects.

Finite difference methods applied to Biot theory is intended to enhance the experimental research mentioned. Very little work has been done in the past regarding Rayleigh wave propagation in porous media. Asymptotic solutions for high and low frequencies were found by Deresiewicz in 1962. However, the author has been unable to find numerical experiments on Rayleigh wave propagation in porous medium valid for intermediate frequency ranges.

The original goal of this thesis was to produce a finite difference code capable of modeling wave propagation in porous media excited by surface tractions. Due to numerical instabilities in discretization of the free surface boundary conditions, the problem modeled was amended to consider body wave propagation in porous media. A two dimensional solution to the problem is discretized using an evenly spaced grid for the "X" and "Y" coordinates, whereby the grid is truncated by an application of homogeneous Dirichlet conditions "relatively" far from the point of application of an incident displacement. Because the spatial discretization is uniform, and center differencing is used throughout, the numerical scheme is second order in space and time. The code is written in C++.

## II. THEORY

Biot theory is one of two popular theoretical methods to model wave propagation in porous media, the other theory assumes the media is viscoelastic. Unlike viscoelastic theory, which is based more upon elasticity theory, Biot theory predicts the existence of three kinds of body waves, two dilatational and one rotational. The first type of dilatational wave involves motions of the skeletal frame and the interstitial fluid which are nearly in phase and for which the attenuation owing to viscous losses is relatively small. The second type of dilatational wave is such that the frame and fluid components are moving largely out of phase. Biot derived two coupled linear differential equations governing the relationship between the displacements of the fluid and the frame. [Ref. 4]

### A. WAVE EQUATIONS

The Biot equations are [Ref. 4]:

$$\rho_{11} \frac{\partial^2 \mathbf{u}}{\partial t^2} + \rho_{12} \frac{\partial^2 \mathbf{U}}{\partial t^2} = (P - \mu) \nabla(\nabla \cdot \mathbf{u}) + \mu \nabla^2 \mathbf{u} + Q \nabla(\nabla \cdot \mathbf{U}) + bF(\omega) \left( \frac{\partial \mathbf{U}}{\partial t} - \frac{\partial \mathbf{u}}{\partial t} \right) \quad (1)$$

$$\rho_{12} \frac{\partial^2 \mathbf{u}}{\partial t^2} + \rho_{22} \frac{\partial^2 \mathbf{U}}{\partial t^2} = Q \nabla(\nabla \cdot \mathbf{u}) + R \nabla(\nabla \cdot \mathbf{U}) - bF(\omega) \left( \frac{\partial \mathbf{U}}{\partial t} - \frac{\partial \mathbf{u}}{\partial t} \right) \quad (2)$$

where

$\mathbf{u}$  = the displacement vector of the solid material;

$\mathbf{U}$  = the displacement vector of the fluid;

$\beta$  = the ratio of the volume of the pores to the total volume of the media;

$\mu$  = the shear modulus of the solid;

$K_b$  = the bulk modulus of the free-draining frame;

$K_f$  = the bulk modulus of the fluid;

$K_r$  = the bulk modulus of the solid;  
 $\rho_f$  = the mass density of the pore fluid;  
 $\rho_r$  = the density of solid material;  
 $\eta$  = fluid viscosity;  
 $\kappa$  = permeability;  
 $\alpha$  = added mass term;  
 $F(\omega)$  = frequency dependent function to account for high frequency attenuation;

such that,

$$Q = [\beta(1 - \beta)K_r - \beta K_b] \div [1 - \beta + \beta \frac{K_r}{K_f} - \frac{K_b}{K_r}]$$

$$R = [\beta^2 K_r] \div [1 - \beta + \beta \frac{K_r}{K_f} - \frac{K_b}{K_r}]$$

$$b = [\eta \beta^2] \div [\kappa]$$

$$P = [(1 - \beta)((1 - \beta) - \frac{K_b}{K_r})K_r + \beta \frac{K_r K_b}{K_f}] \div [1 - \beta + \beta \frac{K_r}{K_f} - \frac{K_b}{K_r}] + \frac{4}{3}\mu$$

$$\rho_{12} = \rho_f \beta (1 - \alpha)$$

$$\rho_{11} = (1 - \beta)\rho_r - \rho_{12}$$

$$\rho_{22} = \rho_f \beta - \rho_{12}$$

**Mathematical notation:** The bold letters denote vectors and the subscripts denote

derivatives with respect to the superscripted variable.

$$\mathbf{U} = \begin{pmatrix} U \\ V \end{pmatrix}; \quad \mathbf{u} = \begin{pmatrix} u \\ v \end{pmatrix};$$

$$\nabla(\nabla \bullet \mathbf{U}) = \begin{pmatrix} U_{xx} + V_{yx} \\ U_{xy} + V_{yy} \end{pmatrix}; \quad \nabla(\nabla \bullet \mathbf{u}) = \begin{pmatrix} u_{xx} + v_{yx} \\ u_{xy} + v_{yy} \end{pmatrix};$$

$$\nabla^2 \mathbf{u} = \begin{pmatrix} u_{xx} + u_{yy} \\ v_{xx} + v_{yy} \end{pmatrix};$$

The  $\mathbf{u}$  and  $\mathbf{U}$  terms in equations (1) and (2) can be isolated as follows:

$$\begin{aligned} \mathbf{U}_{tt}(\rho_{22} - \frac{\rho_{12}^2}{\rho_{11}}) &= Q\nabla(\nabla \bullet \mathbf{u}) + R\nabla(\nabla \bullet \mathbf{U}) - bF(\omega)(\mathbf{U}_t - \mathbf{u}_t) - \{\frac{\rho_{12}}{\rho_{11}} \\ &[(P - \mu)\nabla(\nabla \bullet \mathbf{u}) + \mu\nabla^2 \mathbf{u} + Q\nabla(\nabla \bullet \mathbf{U}) + bF(\omega)(\mathbf{U}_t - \mathbf{u}_t)]\}; \end{aligned} \quad (3)$$

$$\begin{aligned} \mathbf{u}_{tt}(\rho_{12} - \frac{\rho_{22}\rho_{11}}{\rho_{12}}) &= Q\nabla(\nabla \bullet \mathbf{u}) + R\nabla(\nabla \bullet \mathbf{U}) - bF(\omega)(\mathbf{U}_t - \mathbf{u}_t) - \{\frac{\rho_{22}}{\rho_{12}} \\ &[(P - \mu)\nabla(\nabla \bullet \mathbf{u}) + \mu\nabla^2 \mathbf{u} + Q\nabla(\nabla \bullet \mathbf{U}) + bF(\omega)(\mathbf{U}_t - \mathbf{u}_t)]\}; \end{aligned} \quad (4)$$

Rewriting equations (3) and (4) in scalar form:

$$\begin{aligned} \mathbf{U}_{tt} \left( \rho_{22} - \frac{\rho_{12}^2}{\rho_{11}} \right) &= Q(u_{xx} + v_{yx}) + R(U_{xx} + V_{yx}) - bF(\omega)(U_t - u_t) - \left\{ \frac{\rho_{12}}{\rho_{11}} \right. \\ &[(P - \mu)(u_{xx} + v_{yx}) + \mu(u_{xx} + u_{yy}) + Q(U_{xx} + V_{yx}) + bF(\omega)(U_t - u_t)] \} \end{aligned} \quad (5)$$

$$\begin{aligned} \mathbf{V}_{tt} \left( \rho_{22} - \frac{\rho_{12}^2}{\rho_{11}} \right) &= Q(u_{xy} + v_{yy}) + R(U_{xy} + V_{yy}) - bF(\omega)(V_t - v_t) - \left\{ \frac{\rho_{12}}{\rho_{11}} \right. \\ &[(P - \mu)(u_{xy} + v_{yy}) + \mu(v_{xx} + v_{yy}) + Q(U_{xy} + V_{yy}) + bF(\omega)(V_t - v_t)] \} \end{aligned} \quad (6)$$

$$u_{tt}(\rho_{12} - \frac{\rho_{22}\rho_{11}}{\rho_{12}}) = Q(u_{xx} + v_{yx}) + R(U_{xx} + V_{yx}) - bF(\omega)(U_t - u_t) - \{\frac{\rho_{22}}{\rho_{12}}$$

$$[(P - \mu)(u_{xx} + v_{yx}) + \mu(u_{xx} + u_{yy}) + Q(U_{xx} + V_{yx}) + bF(\omega)(U_t - u_t)] \quad (7)$$

$$v_{tt}(\rho_{12} - \frac{\rho_{22}\rho_{11}}{\rho_{12}}) = Q(u_{xy} + v_{yy}) + R(U_{xy} + V_{yy}) - bF(\omega)(V_t - v_t) - \{\frac{\rho_{22}}{\rho_{12}}$$

$$[(P - \mu)(u_{xy} + v_{yy}) + \mu(v_{xx} + v_{yy}) + Q(U_{xy} + V_{yy}) + bF(\omega)(V_t - v_t)] \quad (8)$$

## B. BOUNDARY CONDITIONS

A rectangular grid is used in the X and Y direction. Displacements  $\mathbf{u}$  and  $\mathbf{U}$  are set to zero at all sides of the numerical domain. This creates reflections as body waves strike any of the sides. Originally, on one of the surfaces, a traction free condition was applied which is necessary for the propagation of surface waves and for proper modeling of a porous half space. On this surface, both the stresses and the fluid pressure vanish, resulting in the following boundary conditions:

$$\sigma_{yy}|_{y=0} = (P - 2N)(u_x) + P v_y + Q(U_x + V_y)|_{y=0} = f(x, t); \quad (9)$$

$$\sigma_{xy}|_{y=0} = N(u_y + v_x)|_{y=0} = 0; \quad (10)$$

$$S|_{y=0} = Q(u_x + v_y) + R(U_x + V_y)|_{y=0} = -\beta \times f(x, t); \quad (11)$$

$$U_y + V_x = 0; \quad (12)$$



where  $\sigma$  is the stress tensor and  $S$  is related to the fluid pressure ( $-\beta P$ ), and  $f(x,t)$  is an applied normal force on the surface of the half space. Equations (10) and (12) are the conditions that on the free surface, shear stress is zero for both the solid and the fluid.

### C. SOURCE FUNCTION

The source function used for the half space problem was:

$$F(x, t) = Ae^{-(x-x_0)^2}e^{-(t-t_0)^2}; \quad (13)$$

The source function is Gaussian in shape along the  $x$  grid on the surface.  $x_0$  is the midpoint of the  $x$  grid, while  $t_0$  is the start-up time for the numerical calculations. 'A' is a constant set equal to one pascal.

When it was determined that the discretization for the free surface conditions were unstable, the following two initial states of the displacements were employed to check the accuracy and stability of the code at interior points of the domain.

$$u = \frac{i-i_0}{\sqrt{(i-i_0)^2+(j-j_0)^2}} e^{-\eta[(i-i_0)^2+(j-j_0)^2]} \quad (14)$$

$$v = \frac{j-j_0}{\sqrt{(i-i_0)^2+(j-j_0)^2}} e^{-\eta[(i-i_0)^2+(j-j_0)^2]} \quad (15)$$

$$u = -\frac{j-j_0}{\sqrt{(i-i_0)^2+(j-j_0)^2}} e^{-\eta[(i-i_0)^2+(j-j_0)^2]} \quad (16)$$

$$v = \frac{i-i_0}{\sqrt{(i-i_0)^2+(j-j_0)^2}} e^{-\eta[(i-i_0)^2+(j-j_0)^2]} \quad (17)$$

Equation (14) and (15) were used to check the compressional waves. They can be seen as an initial expansion of the solid portion of the porous medium with two dimensional gaussian shape. Equation (16) and (17) are the cross product of equations (14) and (15) with an out of the page vector ( $\mathbf{k}$ ). They represent an infinitesimal rotation of the solid elements of the two dimensional gaussian distribution of magnitudes, and are used to check the shear wave of the porous medium. Both  $i_o$  and  $j_o$  are set at the center of the grid, and gamma is set equal to 0.1.

### III. PROGRAM ALGORITHM

The program is written in C++. The spatial grid for both the X and the Y axis are chosen to be 0.1 meter, while the time interval,  $\Delta t$  is 0.1 second. The time interval meets the stability requirements to be stated shortly. The Biot equations are scaled prior to the running of the program. Three different sets of Biot parameters were used. Table 1 shows the inputs which remain unchanged for all three parameters sets used.

Omega (fo)	2000 rad/s
F(w)	1
Grid spacing (h)	0.1
Time interval (delta t)	0.1

Table 1. Input Parameters

#### A. FINITE DIFFERENCE SCHEME

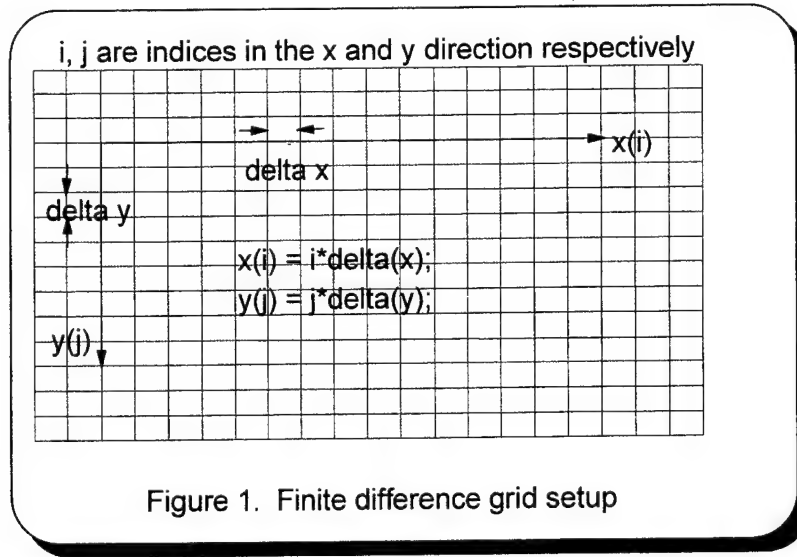
In all the finite difference approximations, center differences are used. Nodal points are found at  $(x_i, y_j)$  where:

$$x_i = i\Delta x; \quad (\text{the horizontal component})$$

$$y_j = j\Delta y; \quad (\text{the vertical component})$$

and the discrete times at which the displacements are found are  $t_n = n\Delta t$ ;

The term  $u_{ij}^n$  therefore refers to  $u(x_i, y_j, t_n)$ ; (See the diagram below).



Some of the difference formula's used are:

$$u_t = \frac{1}{2\Delta t} [u_{ij}^{n+1} - u_{ij}^{n-1}] + O(\Delta t^2);$$

$$u_{xx} = \frac{1}{h^2} [u_{i+1,j}^n - 2u_{i,j}^n + u_{i-1,j}^n] + O(h^2);$$

$$u_{xy} = \frac{1}{4h^2} [u_{i+1,j+1}^n - u_{i+1,j-1}^n + u_{i-1,j-1}^n - u_{i-1,j+1}^n] + O(h^2);$$

The "O" terms are neglected leading to a second order truncation errors throughout the code.

When equations (5)-(8) are differenced in time and space, we may then isolate the unknown displacements at time level 'n+1' as follows:

$$AU_{ij}^{n+1} + Cu_{ij}^{n+1} = E \quad (18)$$

$$BU_{ij}^{n+1} - Du_{ij}^{n+1} = F \quad (19)$$

$$AV_{ij}^{n+1} + Cv_{ij}^{n+1} = G \quad (20)$$

$$BV_{ij}^{n+1} - Dv_{ij}^{n+1} = H \quad (21)$$

The goal is to solve for each grid point's value at the next time level (n+1), to update (or shift time levels), and march forward in steps of  $\Delta t$ .

Solving for the 'n+1' terms from equations (18) through (21) we have:

$$U_{ij}^{n+1} = \frac{DE+CF}{AD+BC} \quad (22)$$

$$u_{ij}^{n+1} = \frac{BE-AF}{AD+BC} \quad (23)$$

$$V_{ij}^{n+1} = \frac{DG+CH}{AD+BC} \quad (24)$$

$$v_{ij}^{n+1} = \frac{BG-AH}{AD+BC} \quad (25)$$

The variables A, B, C, D, E, F, G, H in their respective finite difference form are as follows:

$$A = bF(\omega)\frac{1}{2\Delta t} + \frac{\rho_{22}}{\rho_{12}}bF(\omega)\frac{1}{2\Delta t}; \quad (26)$$

$$B = \frac{1}{\Delta t^2}\left(\rho_{22} - \frac{\rho_{12}^2}{\rho_{11}}\right) + bF(\omega)\frac{1}{2\Delta t} + \frac{\rho_{12}}{\rho_{11}}bF(\omega)\frac{1}{2\Delta t}; \quad (27)$$

$$C = \frac{1}{\Delta t^2}\left(\rho_{12} - \frac{\rho_{22}\rho_{11}}{\rho_{12}}\right) - bF(\omega)\frac{1}{2\Delta t} - \frac{\rho_{22}}{\rho_{12}}bF(\omega)\frac{1}{2\Delta t}; \quad (28)$$

$$D = bF(\omega)\frac{1}{2\Delta t} + \frac{\rho_{12}}{\rho_{11}}bF(\omega)\frac{1}{2\Delta t}; \quad (29)$$

$$E = Q\left\{\frac{1}{h^2}\left(u_{i+1,j}^n - 2u_{i,j}^n + u_{i-1,j}^n\right) + \right.$$

$$\left.\frac{1}{4h^2}\left(v_{i+1,j+1}^n - v_{i-1,j+1}^n + v_{i-1,j-1}^n - v_{i+1,j-1}^n\right)\right\} +$$

$$R\left\{\frac{1}{h^2}\left(U_{i+1,j}^n - 2U_{i,j}^n + U_{i-1,j}^n\right) + \right.$$

$$\left.\frac{1}{4h^2}\left(V_{i+1,j+1}^n - V_{i-1,j+1}^n + V_{i-1,j-1}^n - V_{i+1,j-1}^n\right)\right\} -$$

$$bF(\omega)\frac{1}{2\Delta t}\{u_{i,j}^{n-1} - U_{i,j}^{n-1}\} -$$

$$\frac{\rho_{22}}{\rho_{12}}(P - \mu)\left\{\frac{1}{h^2}\left(u_{i+1,j}^n - 2u_{i,j}^n + u_{i-1,j}^n\right) + \right.$$

$$\frac{1}{4h^2} \left( v_{i+1,j+1}^n - v_{i-1,j+1}^n + v_{i-1,j-1}^n - v_{i+1,j-1}^n \right) \} -$$

$$\frac{\rho_{22}}{\rho_{12}} \mu \left\{ \frac{1}{h^2} \left( u_{i+1,j}^n - 4u_{i,j}^n + u_{i-1,j}^n + u_{i,j+1}^n + u_{i,j-1}^n \right) \right\} -$$

$$\frac{\rho_{22}}{\rho_{12}} Q \left\{ \frac{1}{h^2} \left( U_{i+1,j}^n - 2U_{i,j}^n + U_{i-1,j}^n \right) \right\} +$$

$$\frac{1}{4h^2} \left( V_{i+1,j+1}^n - V_{i-1,j+1}^n + V_{i-1,j-1}^n - V_{i+1,j-1}^n \right) \} -$$

$$\frac{\rho_{22}}{\rho_{12}} bF(\omega) \frac{1}{2\Delta t} \{ u_{i,j}^{n-1} - U_{i,j}^{n-1} \} -$$

$$\frac{1}{\Delta t^2} \left( \rho_{12} - \frac{\rho_{22}\rho_{11}}{\rho_{12}} \right) \left( u_{i,j}^{n-1} - 2u_{i,j}^{n-1} \right); \quad (30)$$

$$F = Q \left\{ \frac{1}{h^2} (u_{i+1,j}^n - 2u_{i,j}^n + u_{i-1,j}^n) \right\} +$$

$$\frac{1}{4h^2} (v_{i+1,j+1}^n - v_{i-1,j+1}^n + v_{i-1,j-1}^n - v_{i+1,j-1}^n) \} +$$

$$R \left\{ \frac{1}{h^2} (U_{i+1,j}^n - 2U_{i,j}^n + U_{i-1,j}^n) \right\} +$$

$$\frac{1}{4h^2} (V_{i+1,j+1}^n - V_{i-1,j+1}^n + V_{i-1,j-1}^n - V_{i+1,j-1}^n) \} -$$

$$bF(\omega) \left( \frac{1}{2\Delta t} \right) \left( u_{i,j}^{n-1} - U_{i,j}^{n-1} \right) -$$

$$\begin{aligned}
& \frac{\rho_{12}}{\rho_{11}}(\mathbf{P} - \boldsymbol{\mu}) \left\{ \frac{1}{h^2} \left( u_{i+1,j}^n - 2u_{i,j}^n + u_{i-1,j}^n \right) + \right. \\
& \left. \frac{1}{4h^2} \left( v_{i+1,j+1}^n - v_{i-1,j+1}^n + v_{i-1,j-1}^n - v_{i+1,j-1}^n \right) \right\} - \\
& \frac{\rho_{12}}{\rho_{11}} \boldsymbol{\mu} \left\{ \frac{1}{h^2} \left( u_{i+1,j}^n - 4u_{i,j}^n + u_{i-1,j}^n + u_{i,j+1}^n + u_{i,j-1}^n \right) \right\} - \\
& \frac{\rho_{12}}{\rho_{11}} \mathbf{Q} \left\{ \frac{1}{h^2} \left( U_{i+1,j}^n - 2U_{i,j}^n + U_{i-1,j}^n \right) + \right. \\
& \left. \frac{1}{4h^2} \left( V_{i+1,j+1}^n - V_{i-1,j+1}^n + V_{i-1,j-1}^n - V_{i+1,j-1}^n \right) \right\} - \\
& \frac{\rho_{12}}{\rho_{11}} \mathbf{bF}(\boldsymbol{\omega}) \left( \frac{1}{2\Delta t} \right) \left( u_{i,j}^{n-1} - U_{i,j}^{n-1} \right) - \\
& \frac{1}{\Delta t^2} \left( \rho_{22} - \frac{\rho_{12}^2}{\rho_{11}} \right) \left( U_{i,j}^{n-1} - 2U_{i,j}^n \right); \tag{31} \\
& \mathbf{G} = \mathbf{Q} \left\{ \frac{1}{4h^2} \left( u_{i+1,j+1}^n - u_{i-1,j+1}^n + u_{i-1,j-1}^n - u_{i+1,j-1}^n \right) + \right. \\
& \left. \frac{1}{h^2} \left( v_{i,j+1}^n - 2v_{i,j}^n + v_{i,j-1}^n \right) \right\} + \\
& \mathbf{R} \left\{ \frac{1}{4h^2} \left( U_{i+1,j+1}^n - U_{i-1,j+1}^n + U_{i-1,j-1}^n - U_{i+1,j-1}^n \right) + \right. \\
& \left. \frac{1}{h^2} \left( V_{i,j+1}^n - 2V_{i,j}^n + V_{i,j-1}^n \right) \right\} - \\
& \mathbf{bF}(\boldsymbol{\omega}) \left( \frac{1}{2\Delta t} \right) \left( v_{i,j}^{n-1} - V_{i,j}^{n-1} \right) -
\end{aligned}$$



$$\begin{aligned}
& \frac{\rho_{22}}{\rho_{12}}(P - \mu) \left\{ \frac{1}{4h^2} \left( u_{i+1,j+1}^n - u_{i-1,j+1}^n + u_{i-1,j-1}^n - u_{i+1,j-1}^n \right) + \right. \\
& \left. \frac{1}{h^2} \left( v_{i,j+1}^n - 2v_{i,j}^n + v_{i,j-1}^n \right) \right\} - \\
& \frac{\rho_{22}}{\rho_{12}} \mu \left\{ \frac{1}{h^2} \left( v_{i+1,j}^n - 4v_{i,j}^n + v_{i-1,j}^n + v_{i,j+1}^n + v_{i,j-1}^n \right) \right\} - \\
& \frac{\rho_{22}}{\rho_{12}} Q \left\{ \frac{1}{4h^2} \left( U_{i+1,j+1}^n - U_{i-1,j+1}^n + U_{i-1,j-1}^n - U_{i+1,j-1}^n \right) + \right. \\
& \left. \frac{1}{h^2} \left( V_{i,j+1}^n - 2V_{i,j}^n + V_{i,j-1}^n \right) \right\} - \\
& \frac{\rho_{22}}{\rho_{12}} bF(\omega) \left( \frac{1}{2\Delta t} \right) \left( v_{i,j}^{n-1} - V_{i,j}^{n-1} \right) - \\
& \frac{1}{\Delta t^2} \left( \rho_{12} - \frac{\rho_{22}\rho_{11}}{\rho_{12}} \right) \left( v_{i,j}^{n-1} - 2v_{i,j}^n \right); \tag{32} \\
& H = Q \left\{ \frac{1}{4h^2} \left( u_{i+1,j+1}^n - u_{i-1,j+1}^n + u_{i-1,j-1}^n - u_{i+1,j-1}^n \right) + \right. \\
& \left. \frac{1}{h^2} \left( v_{i,j+1}^n - 2v_{i,j}^n + v_{i,j-1}^n \right) \right\} + \\
& R \left\{ \frac{1}{4h^2} \left( U_{i+1,j+1}^n - U_{i-1,j+1}^n + U_{i-1,j-1}^n - U_{i+1,j-1}^n \right) + \right. \\
& \left. \frac{1}{h^2} \left( V_{i,j+1}^n - 2V_{i,j}^n + V_{i,j-1}^n \right) \right\} -
\end{aligned}$$

$$\begin{aligned}
& bF(\omega) \left( \frac{1}{2\Delta t} \right) \left( v_{ij}^{n-1} - V_{ij}^{n-1} \right) - \\
& \frac{\rho_{12}}{\rho_{11}} (p - \mu) \left\{ \frac{1}{4h^2} \left( u_{i+1,j+1}^n - u_{i-1,j+1}^n + u_{i-1,j-1}^n - u_{i+1,j-1}^n \right) + \right. \\
& \left. \frac{1}{h^2} \left( V_{i,j+1}^n - 2V_{ij}^n + V_{i,j-1}^n \right) \right\} - \\
& \frac{\rho_{12}}{\rho_{11}} \mu \left\{ \frac{1}{h^2} \left( v_{i+1,j}^n - 4v_{ij}^n + v_{i-1,j}^n + v_{i,j+1}^n + v_{i,j-1}^n \right) \right\} - \\
& \frac{\rho_{12}}{\rho_{11}} Q \left\{ \frac{1}{4h^2} \left( U_{i+1,j+1}^n - U_{i-1,j+1}^n + U_{i-1,j-1}^n - U_{i+1,j-1}^n \right) + \right. \\
& \left. \frac{1}{h^2} \left( V_{i,j+1}^n - 2V_{ij}^n + V_{i,j-1}^n \right) \right\} - \\
& \frac{\rho_{12}}{\rho_{11}} bF(\omega) \left( \frac{1}{2\Delta t} \right) \left( v_{ij}^{n-1} - V_{ij}^{n-1} \right) - \\
& \frac{1}{\Delta t^2} \left( \rho_{22} - \frac{\rho_{12}^2}{\rho_{11}} \right) \left( V_{ij}^{n-1} - 2V_{ij}^n \right); \tag{33}
\end{aligned}$$

Second order finite difference forms of the boundary conditions equations (9)

through (12) are given by:

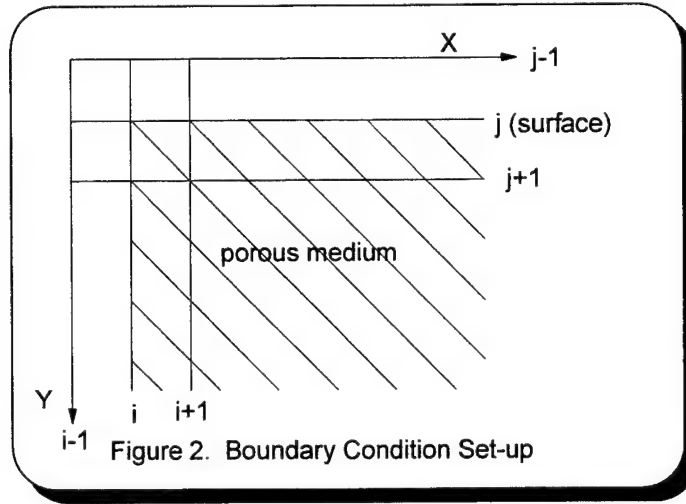
$$\begin{aligned}
& (P - 2N) \left\{ \frac{1}{2h} (u_{i+1,j}^n - u_{i-1,j}^n) \right\} + P \left\{ \frac{1}{2h} \left( v_{i,j+1}^n - v_{i,j-1}^n \right) \right\} + \\
& Q \left\{ \frac{1}{2h} (U_{i+1,j}^n - U_{i-1,j}^n + V_{i,j+1}^n - V_{i,j-1}^n) \right\} = f_i^n; \tag{34}
\end{aligned}$$

$$N\left\{\frac{1}{2h}\left(u_{i,j+1}^n - u_{i,j-1}^n + v_{i+1,j}^n - v_{i-1,j}^n\right)\right\} = 0; \quad (35)$$

$$Q\left\{\frac{1}{2h}\left(u_{i+1,j}^n - u_{i-1,j}^n + v_{i,j+1}^n - v_{i,j-1}^n\right) + R\left\{\frac{1}{2h}\left(U_{i+1,j}^n - U_{i-1,j}^n + V_{i,j+1}^n - V_{i,j-1}^n\right) = -\beta f_i^n; \quad (36)$$

$$\frac{1}{2}\left(U_{i,j+1}^n - U_{i,j-1}^n + V_{i+1,j}^n - V_{i-1,j}^n\right) = 0; \quad (37)$$

Equations (34) through (37) give the means to calculate the 'j-1' terms exterior to the boundary surface (see Figure (2)), which are in turn substituted into equations (30) through (33) to find the values of  $\mathbf{u}$  and  $\mathbf{U}$  along the free surface boundary.



## B. SCALING

Only two parameters need to be scaled in the Biot equations, time and length. The equations for the displacements are linear, therefore their scaling is determined by the magnitude of the applied force on the free surface or by the initial displacements

assigned. The time scale chosen is  $\omega$  in rad/sec, while the length scale used is  $L=1$  meter. These scales lead to the following relationships:

$$x_s = \frac{x}{L}; \quad x = Lx_s; \quad \frac{\partial}{\partial x} = \frac{1}{L} \frac{\partial}{\partial x_s}; \quad (38)$$

$$t_s = \omega t; \quad t = \frac{t_s}{\omega}; \quad \frac{\partial}{\partial t} = \omega \frac{\partial}{\partial t_s}. \quad (39)$$

In addition to scaling, a constant term of  $\frac{L^2}{\mu}$  is multiplied across each equation. The result is a constant multiplier  $\frac{\omega^2 L^2}{\mu}$  to all terms involving second derivatives with respect to time,  $\frac{\omega L^2}{\mu}$  to all first derivatives in time, and  $\frac{1}{\mu}$  to all second derivatives in  $x$  or  $y$ .

### C. STABILITY

The system of equations (18) to (21) was found to be stable provided that

$$\Delta t \leq h \div \left( V_{p_c}^2 + V_s^2 \right)^{\frac{1}{2}}; \quad (40)$$

$$V_{p_c} = \sqrt{\frac{K_c + 4\mu/3}{\rho}}; \quad (41)$$

$$V_s = \sqrt{\frac{\mu}{\rho}} \quad (42)$$

$K_c$  = bulk modulus of the saturated medium

$$= \beta K_f + (1 - \beta) K_r;$$

$$\rho = \beta \rho_f + (1 - \beta) \rho_r;$$

$\mu$  = shear modulus of the frame;

$h$  = the grid interval in both  $x$  and the  $y$  direction;

$\Delta t$  = the time step;

$V_{pc}$  =the saturated velocity of the fast compressional wave;

$V_s$  =the shear wave velocity;

Equation (40) is the stability condition used in finite-difference algorithms

involving wave propagation for elastic media. [Ref. 5] For porous medium, equation

(40) is also valid because the saturated velocity of the fast compressional velocity in the

porous elastic solid is normally much less than the compressional velocity of the purely

elastic solid.

After scaling, the stability equation (40) becomes:

$$\Delta t_s \leq (\omega L h) \div \sqrt{V_{pc}^2 + V_s^2}; \quad (43)$$

#### D. PARAMETERS

The parameters used are shown in the table below.

	Units	Stoll & Kan	ARL:UT	ARL:UT mod
<b>Bulk parameters</b>				
porosity	...	0.47	0.4	0.2
grain density	kg/m <sup>3</sup>	2650	2650	2400
liquid density	kg/m <sup>3</sup>	1000	1000	1000
grain bulk modulus	Pa	3.6E+10	7E+09	7E+09
liquid bulk modulus	Pa	2E+09	2.25E+09	2.25E+09
<b>Liquid motion</b>				
viscosity	kg/m s	1E-03	1E-03	0
permeability	m <sup>2</sup>	1E-10	4.99E-11	4.99E-11
pore size	m	1E-05	4.99E-05	4.99E-05
virtual mass constant	...	1.25	1.75	1.75
<b>Frame response</b>				
frame shear modulus	Pa	2.61E+07	2.61E+07	2.61E+07
shear log decrement	...	0.15	0.15	0.15
frame bulk modulus	Pa	4.36E+07	5.3E+09	5.3E+09
bulk log decrement	...	0.15	0.15	0.15

Table 2. Biot model parameters "From Ref. 5 and 6"

The Stoll and Kan parameters and the ARL:UT parameters are taken from [Ref. 6].

ARL:UT parameters are believed to be the better parameters to use based on the experiments performed by Chotiros, ARL University of Texas at Austin. The modified ARL:UT is the same as ARL:UT parameters except the fluid viscosity is set to zero, eliminating any damping in the system, and smaller grain density and lower porosity ratios are used. The wave speeds calculated using the above parameters are shown in Table 3.

	Stoll & Kan	ARL:UT	ARL:UT mod
Fast P wave speed	1485.14m/s	1694.8m/s	1676.7 m/s
Slow P wave speed	56.21m/s	192.83 m/s	1066.8 m/s
Sheer speed	119.24m/s	114.7 m/s	114.07 m/s

Table 3. Wave Speeds

Equations used to calculate the compressional and shear wave speeds are [Ref. 7]:

$$P_{\text{fast}} = \sqrt{\text{Real}((2AH)/(B - jf - \text{Del}))} ;$$

$$P_{\text{slow}} = \sqrt{\text{Real}((2AH)/(B - if + \text{Del}))} ;$$

$$S = \sqrt{\text{Real}(\mu((\rho_{22}/\rho) - jf)/(\rho(C - jf)))} ;$$

where,

$$H = P + 2Q + R;$$

$$A = (PR - Q^2)/H^2 ;$$

$$B = (\rho_{11}R + \rho_{22}P - 2\rho_{12}Q)/(\rho H);$$

$$C = (\rho_{11}\rho_{22} - \rho_{12}^2)/\rho^2;$$

$$\text{Del} = \sqrt{(B - jf)^2 - 4A(C - jf)} ;$$

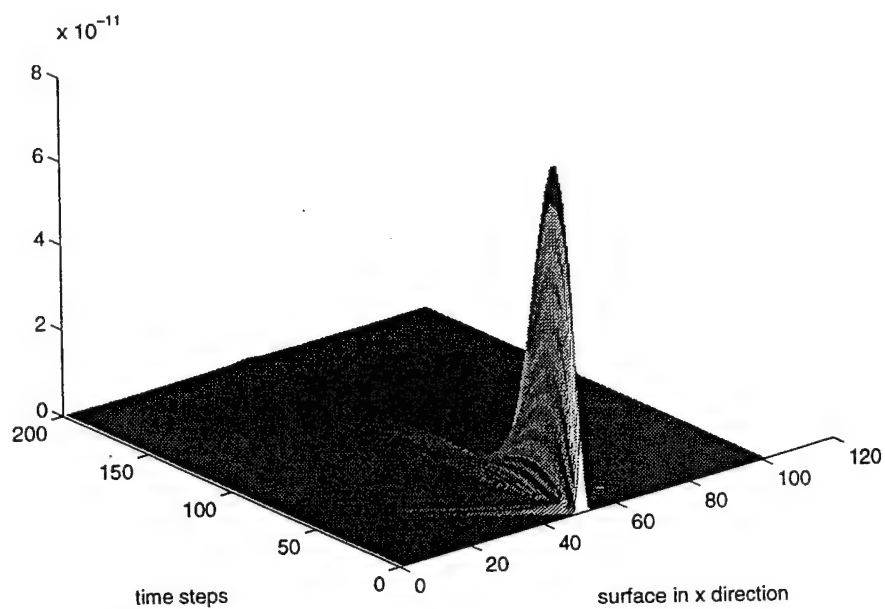
$$f = \mu\beta/(\kappa\rho\omega).$$

## E. DISCUSSION

The source was applied to the finite difference model only once at the initial time level in an attempt to model an instantaneous point force surface traction on a porous half-space. Because of the porous parameters used, the shear speed was small compared to the fast compressional wave. The large difference in speeds is assumed to be the cause of a numerical instability at the free surface boundary. An instability of this form was reported in the work of Ilan and Loewenthal in 1976 [Ref. 8]. To test this hypothesis the value of the shear modulus was increased to within the reported stability region of center-differencing of the free surface conditions, but still the code was unstable. Alternative differencing of the free surface conditions proved futile, so a decision was made to drop the free surface altogether and apply homogeneous Dirichlet Boundary Condition on all sides of the numerical domain. This numerical problem identifies an area of future research.

The Stoll & Kan parameters demonstrate short propagation distances due to the relatively large frequency and high attenuation of the media. (Figure (3)) The ARL:UT which neglects fluid viscosity gives a much better contrast for the fast compressional wave propagation as reflections off the sides can also be observed. (Figures (4) and (5)) The fast and the slow compressional wave are visible using the ARL:UT mod parameters. (Figures (6) and (7)) From Figure 7, the fast and slow compressional wave speeds can be calculated using equation (44).

Solid displacement, Stoll & Kan



Fluid displacement, Stoll & Kan

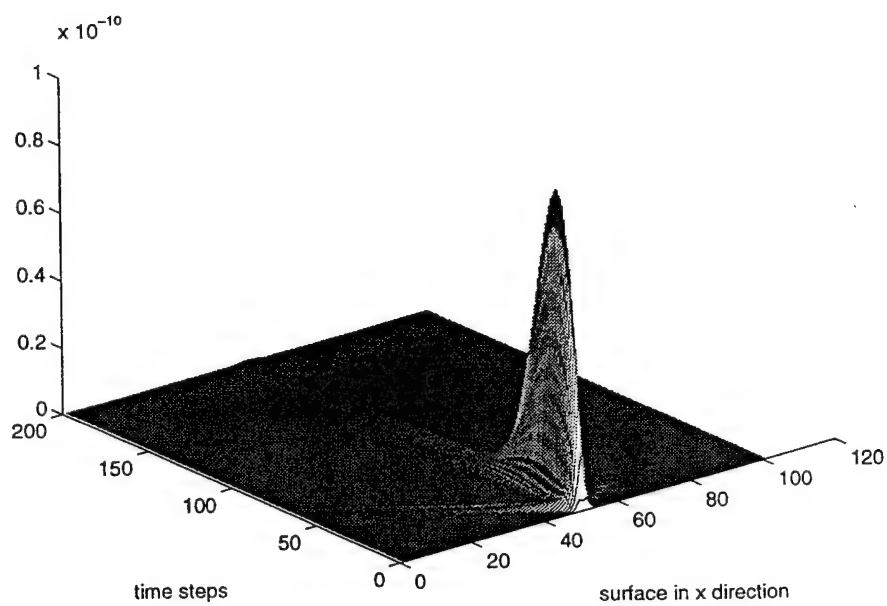
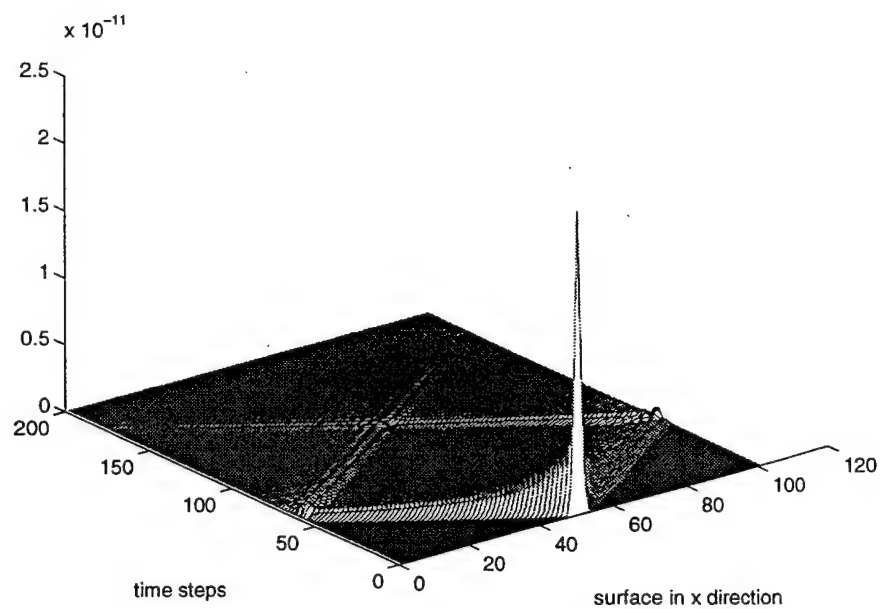


Figure 3. Solid and Fluid Displacement, Stoll & Kan



Solid displacement, ARL:UT



Fluid displacement, ARL:UT

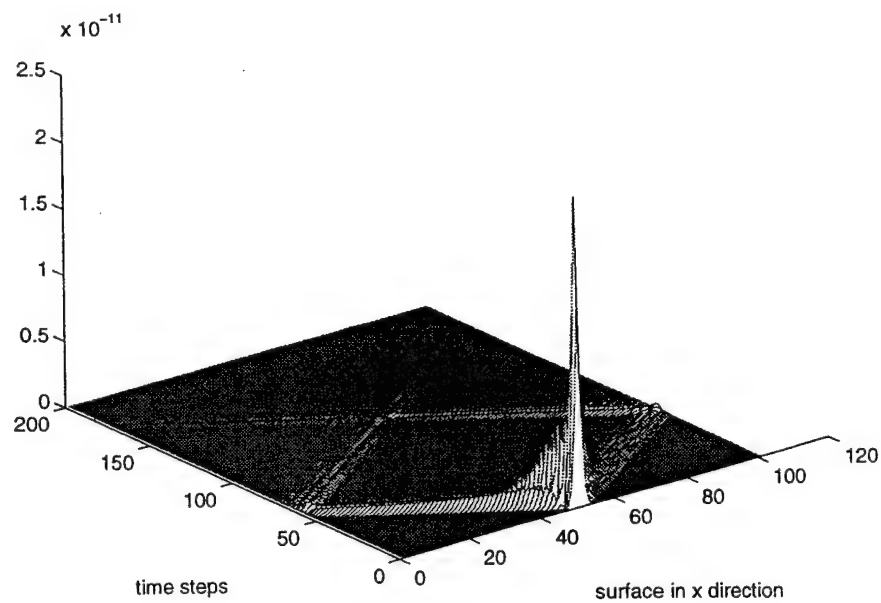


Figure 4. Solid and Fluid Displacement, ARL:UT

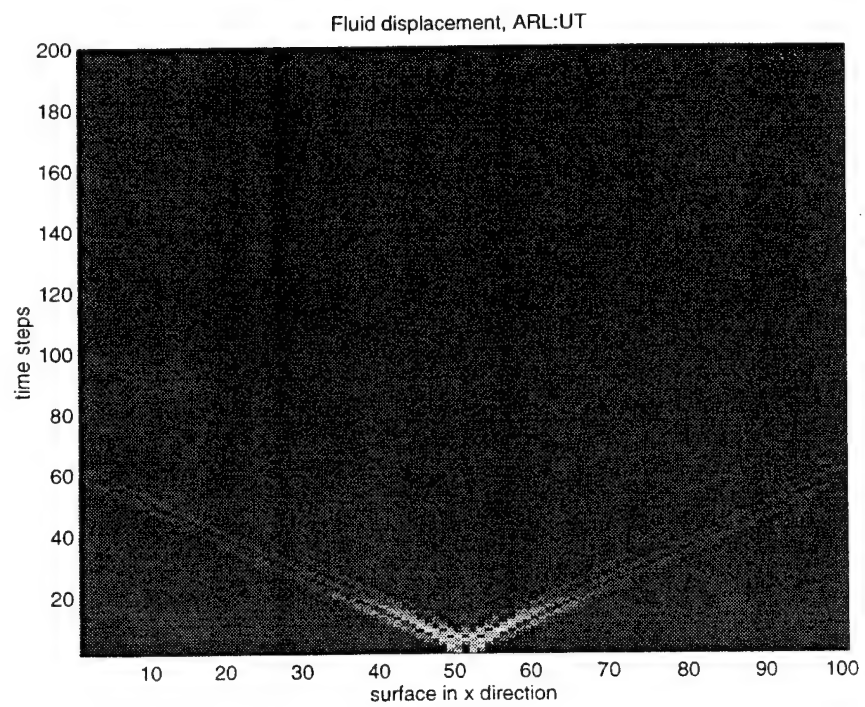
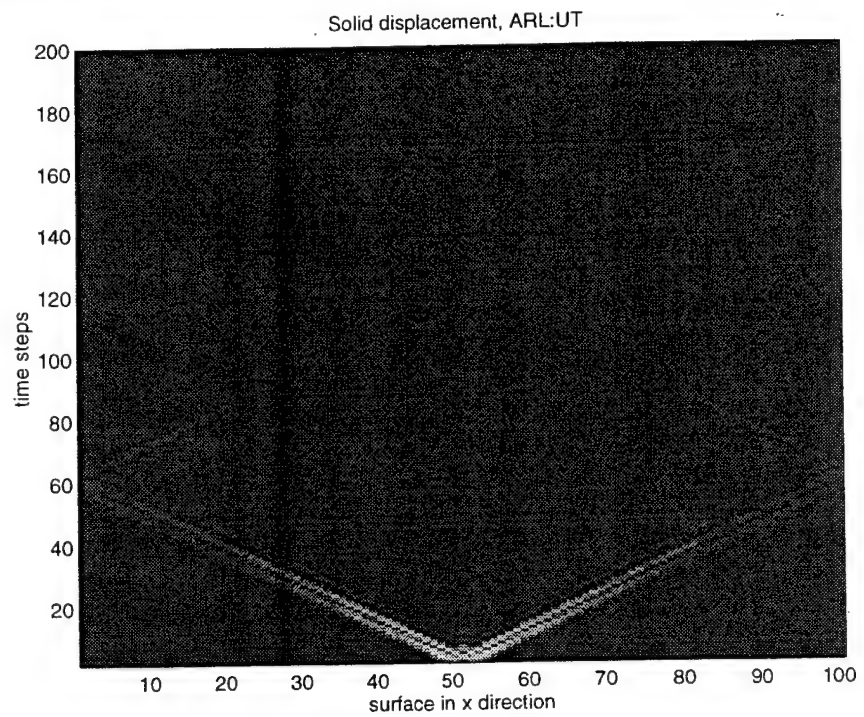
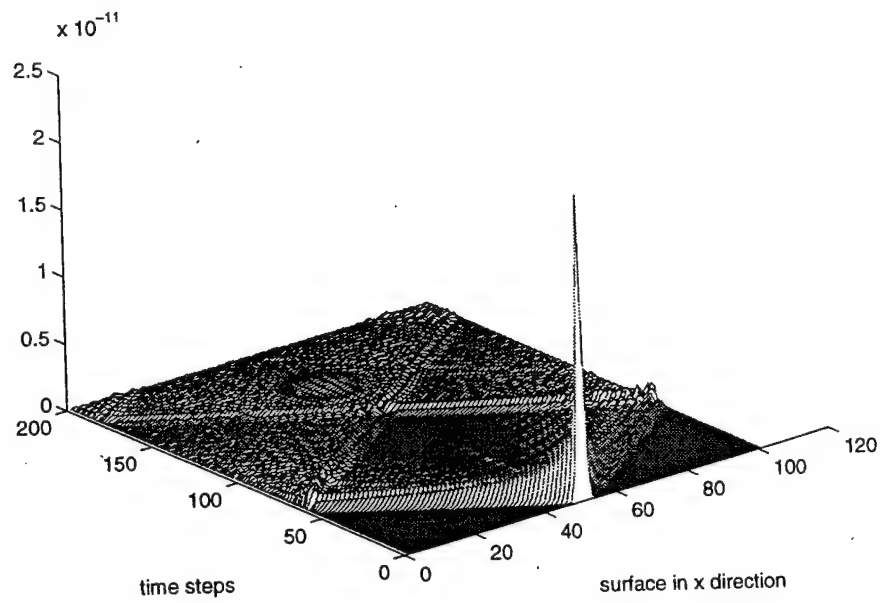


Figure 5. Top View - Solid and Fluid Displacement, ARL:UT

Solid displacement, ARL:UT mod



Fluid displacement, ARL:UT mod

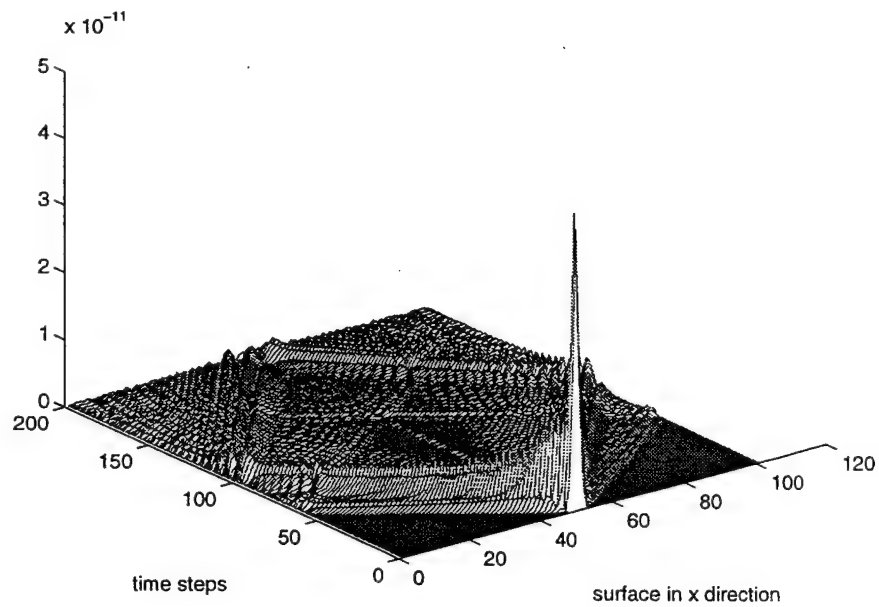


Figure 6. Solid and Fluid Displacement, ARL:UT Mod

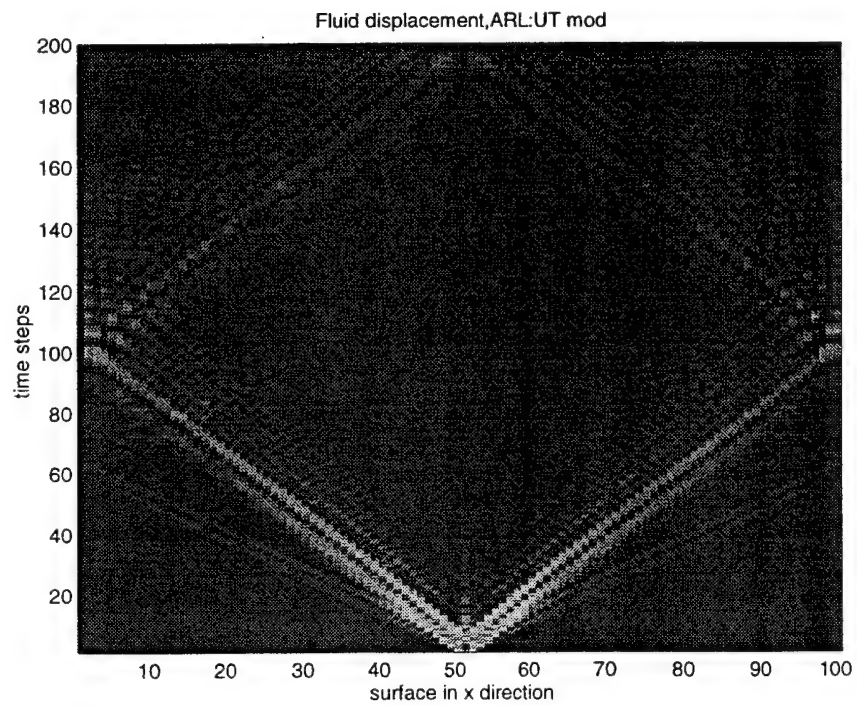
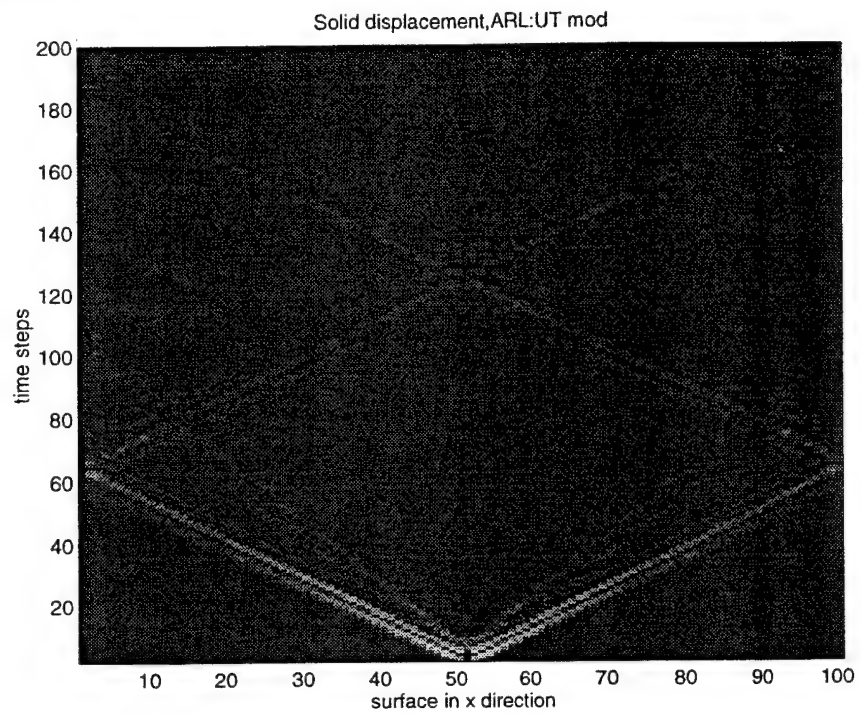


Figure 7. Top View - Solid and Fluid Displacement, ARL:UT Mod

$$C = \frac{\omega \Delta h}{\Delta t} ; \quad \omega = 2000 \text{ rad/sec}; \quad L=1 \text{ m.} \quad (44)$$

For the fast compressional wave speed, it traveled 50 grids in about 60 time level giving us a speed of 1666 m/s. The slow compressional wave speed traveled 50 grids in 100 time level giving us a speed of 1000 m/s.

To check the accuracy and stability of the code at interior points of the domain, equations (14) through (17) were used and the results shown in Figure (8) and (9). In Figure (8), the cylindrical spreading show a propagation of approximately 80 grids in 100 time level for a 1600 m/s fast compressional wave speed. In Figure (9), no shear propagation in the fluid is seen as expected for fluids do not support shear propagation. For the solid, shear speed propagated approximately 11 grids in 200 time level giving us a shear wave speed of 110 m/s. It is extremely difficult to distinguish the slow wave propagation from that of the fast wave in Figure (8). However, due to the fact that the frame and fluid components of the slow wave are moving largely out of phase and the fast wave moves nearly in phase, a plot of relative speed between the frame and the fluid would make the slow wave more visible. (Figure (10)). In Figure (10), the slow wave is seen to propagate to about 50 grids in 100 time levels for a slow speed of 1000 m/s.

All of the figures shown and numbers calculated have propagation speeds that match well with the theory shown in Table (3).

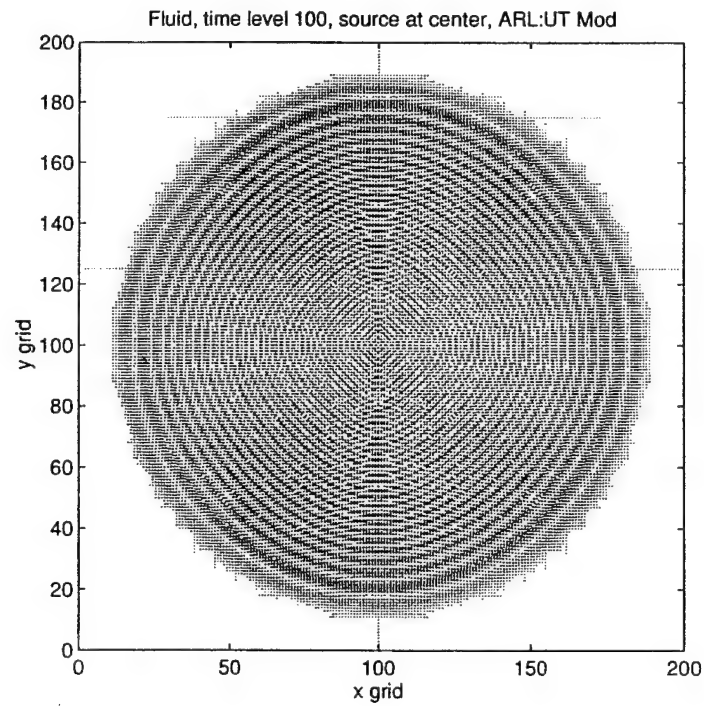
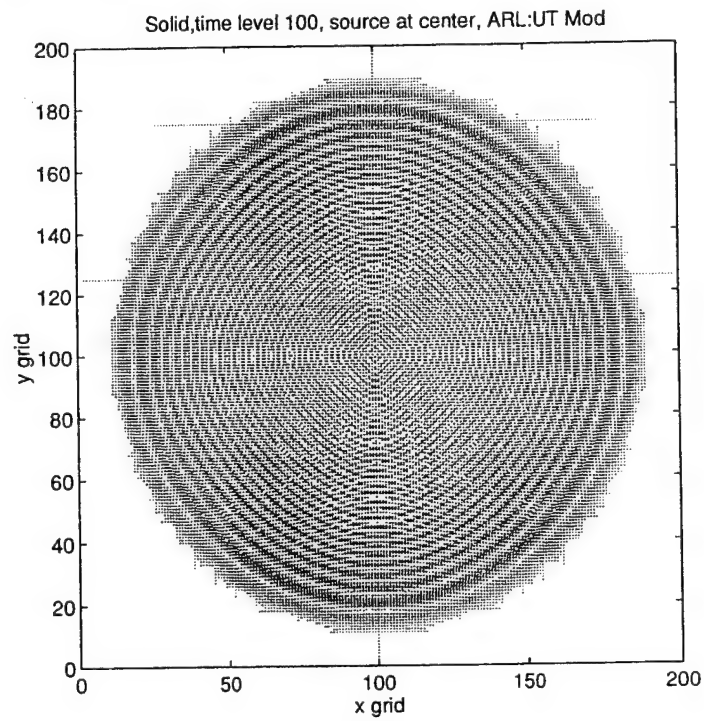


Figure 8. Compressional Solid and Fluid Displacement, ARL:UT Mod

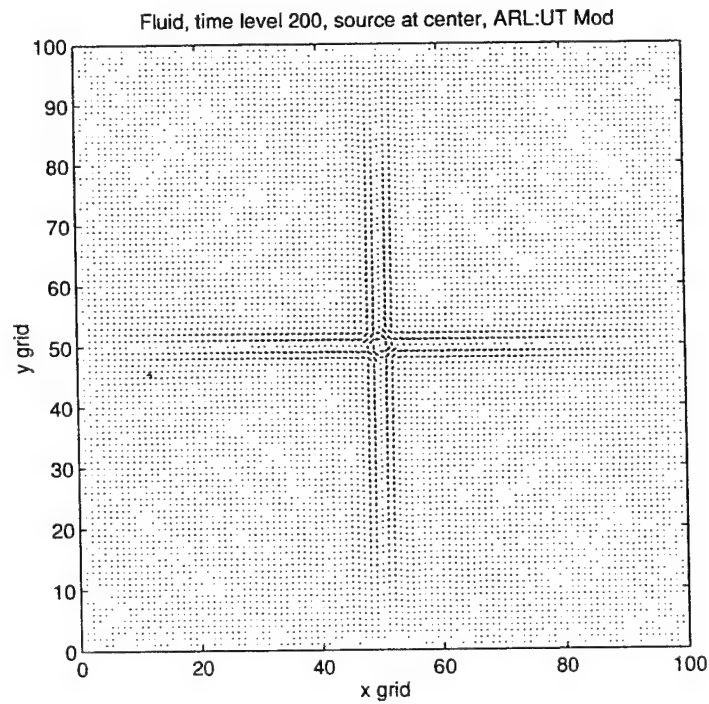
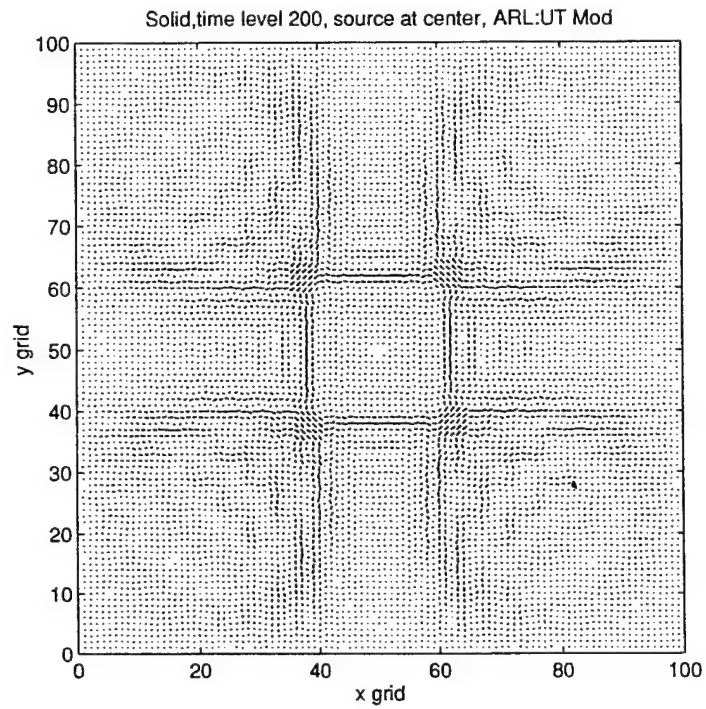
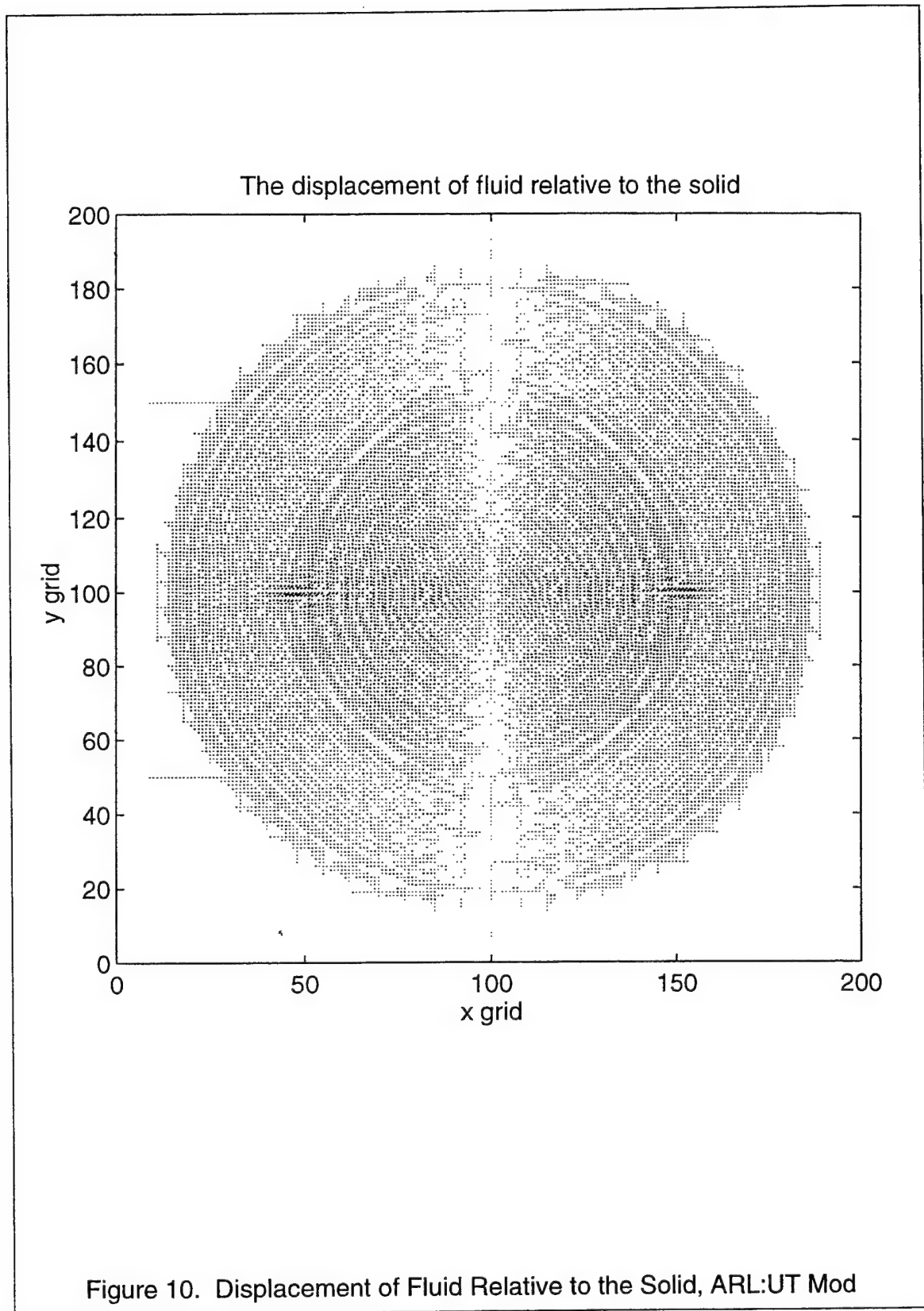


Figure 9. Shear Solid and Fluid Displacement, ARL:UT Mod





#### IV. CONCLUSION

The propagation of the fast compressional waves can be clearly seen in all three parameter sets used. The program behaved as expected concerning the body waves and their speeds matched well with theory. The different parameters used have shown the sensitivity of Biot parameters in wave propagation.

One area that should be pursued is to determine a stable free surface boundary condition difference operator so that Rayleigh wave propagation may be modeled. Another improvement on the current code would be to include absorbing boundary conditions on the sides and the bottom, to better model a semi-infinite domain.



## APPENDIX PROGRAM CODE

```

/*****
/* Thesis Program for Wave Propagation */
/* Programmer: Jonah Shen */
/* Date: June 1995 */
/* Language: C, beta, scaled */
*****/

#include <stdio.h>
#include <math.h>

/* Initialization of variables and constants */

float beta = 0.47; /* beta is the ratio of the vol of */
/* the pore to total vol of element */
float Mu = 2.61e7; /* shear modulus, Pa */
float rhor = 2650.0; /* grain density, Kg/m^3 */
float rhof = 1000.0; /* fluid density, Kg/m^3 */
float Kb = 4.36e7; /* bulk modulus of frame, Pa */
float Kr = 3.6e10; /* bulk modulus of solid, Pa */
float Kf = 2.0e9; /* bulk modulus of fluid, Pa */
float N = 1e-3; /* liquid viscosity, kg/m s */
float K = 1e-10; /* liquid permeability, m^2 */
float delT = 0.1; /* delta t */
float Fw = 1.0; /* forcing function */
float h = 0.1; /* step size */
float alpha = 3.0;
float w = 2000.0;

float a,Q,R,P,b,rho12,rho11,rho22,AA,BB,CC,DD,EE,FF,GG,HH,II,JJ,KK,LL;
float MM,NN,y,f;
float Aa,Bb,Cc,Dd,Ee,Ff,Gg,Hh,Ii,Jj,Kk,Ll,Mm,Nn,Oo,Pp,Qq,Rr,ans;
float aA,bB,cC,dD,eE,fF,gG,hH,iI,jJ,kK,lL,mM,nN,oO,pP,qQ,rR;
int n,i,j,ind,time,tt;

/*****
/* Defining Vectors for finite difference */
/* Lower case is displacement of points in the skeletal frame */
/* Upper case is displacement of fluid */
/* Each letter will be follow by 3 numbers, the first number */
/* represent time second represent x direction, third represent */

```

```

/* y direction */
/*****

float u[3][51][51];
float v[3][51][51];
float U[3][51][51];
float V[3][51][51];
float sol[300][51];
float flu[300][51];

/* Declare Function Prototype */

float FEE(float Aa,float Bb,float Cc,float Dd,float Ee,float Ff,float Gg,
float Hh,float Ii,float Jj,float Kk,float Ll,float Mm,float Nn,
float Oo,float Pp,float Qq,float Rr);
float FFF(float Aa,float Bb,float Cc,float Dd,float Ee,float Ff,float Gg,
float Hh,float Ii,float Jj,float Kk,float Ll,float Mm,float Nn,
float Oo,float Pp,float Qq,float Rr);
float FGG(float aA,float bB,float cC,float dD,float eE,float fF,float gG,
float hH,float iI,float jJ,float kK,float lL,float mM,float nN,
float oO,float pP,float qQ,float rR);
float FHH(float aA,float bB,float cC,float dD,float eE,float fF,float gG,
float hH,float iI,float jJ,float kK,float lL,float mM,float nN,
float oO,float pP,float qQ,float rR);

main()
{
a = (1-beta+(beta*Kr/Kf)-(Kb/Kr));
Q = (beta*(1-beta)*Kr-beta*Kb)/a;
R = beta*beta*Kr/a;
P = ((1-beta)*((1-beta)-Kb/Kr)*Kr+(beta*Kr*Kb/Kf))/a + 4*Mu/3;
b = N*beta*beta/K;
rho12 = rhof*beta*(1-alpha);
rho11 = (1-beta)*rhor-rho12;
rho22 = rhof*beta-rho12;
AA = b*Fw*w/(2*delT*Mu) + rho22*b*Fw*w/(rho12*2*delT*Mu);
BB = (w*w/(delT*delT*Mu))*(rho22-(rho12*rho12/rho11))+b*Fw*w/(2*delT*Mu)+
b*Fw*w*rho12/(2*delT*Mu*rho11);
CC = (w*w/(delT*delT*Mu))*(rho12-(rho22*rho11/rho12))-b*Fw*w/(2*delT*Mu)-
b*Fw*w*rho22/(2*delT*Mu*rho12);
DD = b*Fw*w/(2*delT*Mu)+rho12*b*Fw*w/(rho11*2*delT*Mu);
/* Initialization of the arrays */

```

```

for (n=0;n<=2;n++)
{
    for (i=0;i<=50;i++)
    {
        for (j=0;j<=50;j++)
        {
            u[n][i][j] = 0.0;
            v[n][i][j] = 0.0;
            U[n][i][j] = 0.0;
            V[n][i][j] = 0.0;
        }
    }
}

/* Loops */

time=200;
ind = 0;
n=1;

/* Boundary Conditions */

for (i=1;i<=49;i++)
{
    j=1;
    y=1.0;
    f=exp(-(i-25)*(i-25));

    U[n][i][j-1]=U[n][i][j+1]+V[n][i+1][j]-V[n][i-1][j];
    u[n][i][j-1]=u[n][i][j+1]-v[n][i-1][j]+v[n][i+1][j];

    II=-((2*h*f*y)+((P-2*Mu)*(u[n][i+1][j]-u[n][i-1][j])+P*v[n][i][j+1]
        +Q*(V[n][i][j+1]-U[n][i-1][j]+U[n][i+1][j])));
    JJ=(beta*2*h*f*y)+Q*(v[n][i][j+1]-u[n][i-1][j]+u[n][i+1][j])+
        R*(V[n][i][j+1]-U[n][i-1][j]+U[n][i+1][j]);

    v[n][i][j-1]=(II*R - Q*JJ)/(P*R - Q*Q);
    V[n][i][j-1]=(Q*II - P*JJ)/(Q*Q - P*R);
}

while (ind < time)
{
    for (i=1;i<=49;i++)
    {
        for (j=1;j<=49;j++)
        {
            Aa=u[n][i+1][j];

```

```

Bb=u[n][i][j];
Cc=u[n][i-1][j];
Dd=u[n-1][i][j];
Ee=u[n][i][j+1];
Ff=u[n][i][j-1];
Gg=v[n][i-1][j+1];
Hh=v[n][i-1][j-1];
Ii=v[n][i+1][j+1];
Jj=v[n][i+1][j-1];
Kk=U[n][i+1][j];
Ll=U[n][i][j];
Mm=U[n][i-1][j];
Nn=U[n-1][i][j];
Oo=V[n][i+1][j+1];
Pp=V[n][i-1][j+1];
Qq=V[n][i-1][j-1];
Rr=V[n][i+1][j-1];
aA=u[n][i+1][j+1];
bB=u[n][i-1][j+1];
cC=u[n][i-1][j-1];
dD=u[n][i+1][j-1];
eE=v[n][i][j+1];
fF=v[n][i][j];
gG=v[n][i][j-1];
hH=v[n-1][i][j];
iI=v[n][i+1][j];
jJ=v[n][i-1][j];
kK=U[n][i+1][j+1];
lL=U[n][i-1][j+1];
mM=U[n][i-1][j-1];
nN=U[n][i+1][j-1];
oO=V[n][i][j+1];
pP=V[n][i][j];
qQ=V[n][i][j-1];
rR=V[n-1][i][j];

```

```

EE=FEE(Aa,Bb,Cc,Dd,Ee,Ff,Gg,Hh,Ii,Jj,Kk,Ll,Mm,Nn,Oo,Pp,Qq,Rr);
FF=FFF(Aa,Bb,Cc,Dd,Ee,Ff,Gg,Hh,Ii,Jj,Kk,Ll,Mm,Nn,Oo,Pp,Qq,Rr);
GG=FGG(aA,bB,cC,dD,eE,fF,gG,hH,iI,jJ,kK,lL,mM,nN,oO,pP,qQ,rR);
HH=FHH(aA,bB,cC,dD,eE,fF,gG,hH,iI,jJ,kK,lL,mM,nN,oO,pP,qQ,rR);

```

```

/* Calculating the n+1 values */

```

```

        u[n+1][i][j]=(BB*EE-AA*FF)/(BB*CC+AA*DD);
        v[n+1][i][j]=(BB*GG-AA*HH)/(BB*CC+AA*DD);
        U[n+1][i][j]=(DD*EE+CC*FF)/(BB*CC+AA*DD);
        V[n+1][i][j]=(DD*GG+CC*HH)/(BB*CC+AA*DD);
    }
}

for (i=0;i<=50;i++)
{
    for (j=0;j<=50;j++)
    {
        /* Updating the grid for next time level */

        u[n-1][i][j]=u[n][i][j];
        u[n][i][j]=u[n+1][i][j];
        v[n-1][i][j]=v[n][i][j];
        v[n][i][j]=v[n+1][i][j];
        U[n-1][i][j]=U[n][i][j];
        U[n][i][j]=U[n+1][i][j];
        V[n-1][i][j]=V[n][i][j];
        V[n][i][j]=V[n+1][i][j];
    }
}

for (i=1;i<=49;i++)
{
    sol[ind][i]=sqrt(v[2][i][1]*v[2][i][1]+u[2][i][1]*u[2][i][1]);
    flu[ind][i]=sqrt(V[2][i][1]*V[2][i][1]+U[2][i][1]*U[2][i][1]);
}

ind = ind + 1;

}

for (tt=0;tt<time;tt++)
{
    for (i=0;i<=50;i++)
        printf("\n%d\t%d\t%g\t%g",tt,i,sol[tt][i],flu[tt][i]);
}

/*for (i=1;i<=49;i++)
{

```

```

        for (j=1;j<=49;j++)
        {
            printf("\n%d\t%d\t%g\t%g\t%g\t%g",i,j,u[n][i][j],v[n][i][j],
                U[n][i][j],V[n][i][j]);
        }
    }*/

return 0;
}

/* Declared Function Definition */

float FEE(float Aa,float Bb,float Cc,float Dd,float Ee,float Ff,float Gg,
    float Hh,float Ii,float Jj,float Kk,float Ll,float Mm,float Nn,
    float Oo,float Pp,float Qq,float Rr)
{
    a = (1-beta+(beta*Kr/Kf)-(Kb/Kr));
    Q = (beta*(1-beta)*Kr-beta*Kb)/a;
    R = beta*beta*Kr/a;
    P = ((1-beta)*((1-beta)-Kb/Kr)*Kr+(beta*Kr*Kb/Kf))/a + 4*Mu/3;
    b = N*beta*beta/K;
    rho12 = rhoF*beta*(1-alpha);
    rho11 = (1-beta)*rhoR-rho12;
    rho22 = rhoF*beta-rho12;
    ans = Q/Mu*((Aa-2*Bb+Cc)/(h*h)+(Ii-Gg+Hh-Jj)/(4*h*h)) +
        R/Mu*((Kk-2*Ll+Mm)/(h*h)+(Oo-Pp+Qq-Rr)/(4*h*h)) -
        b*Fw*w*((Dd-Nn)/(2*delT*Mu)) -
        rho22*(P-Mu)/(Mu*rho12)*((Aa-2*Bb+Cc)/(h*h)+(Ii-Gg+Hh-Jj)/(4*h*h)) -
        rho22/rho12*(Aa-4*Bb+Cc+Ee+Ff)/(h*h) -
        rho22*Q/(rho12*Mu)*((Kk-2*Ll+Mm)/(h*h)+(Oo-Pp+Qq-Rr)/(4*h*h)) -
        rho22*b*Fw*w*(Dd-Nn)/(rho12*2*delT*Mu) -
        (Dd-2*Bb)*w*w*(rho12-((rho22*rho11)/rho12))/(delT*delT*Mu);
    return ans;
}

float FFF(float Aa,float Bb,float Cc,float Dd,float Ee,float Ff,float Gg,
    float Hh,float Ii,float Jj,float Kk,float Ll,float Mm,float Nn,
    float Oo,float Pp,float Qq,float Rr)
{
    a = (1-beta+(beta*Kr/Kf)-(Kb/Kr));
    Q = (beta*(1-beta)*Kr-beta*Kb)/a;
    R = beta*beta*Kr/a;

```



```

P = ((1-beta)*((1-beta)-Kb/Kr)*Kr+(beta*Kr*Kb/Kf))/a + 4*Mu/3;
b = N*beta*beta/K;
rho12 = rhoF*beta*(1-alpha);
rho11 = (1-beta)*rhoR-rho12;
rho22 = rhoF*beta-rho12;
ans = Q/Mu*((Aa-2*Bb+Cc)/(h*h)+(Li-Gg+Hh-Jj)/(4*h*h)) +
      R/Mu*((Kk-2*Ll+Mm)/(h*h)+(Oo-Pp+Qq-Rr)/(4*h*h)) -
      b*Fw*w*((Dd-Nn)/(2*delT*Mu)) -
      rho12*(P-Mu)/(rho11*Mu)*((Aa-2*Bb+Cc)/(h*h)+(Li-Gg+Hh-Jj)/(4*h*h)) -
      rho12/rho11*(Aa-4*Bb+Cc+Ee+Ff)/(h*h) -
      rho12*Q/(rho11*Mu)*((Kk-2*Ll+Mm)/(h*h)+(Oo-Pp+Qq-Rr)/(4*h*h)) -
      rho12*b*Fw*w*(Dd-Nn)/(rho11*2*delT*Mu) -
      (Nn-2*Ll)*w*w*(rho22-((rho12*rho12)/rho11))/(delT*delT*Mu);
return ans;
}

```

```

float FGG(float aA,float bB,float cC,float dD,float eE,float fF,float gG,
          float hH,float iI,float jJ,float kK,float lL,float mM,float nN,
          float oO,float pP,float qQ,float rR)
{
a = (1-beta+(beta*Kr/Kf)-(Kb/Kr));
Q = (beta*(1-beta)*Kr-beta*Kb)/a;
R = beta*beta*Kr/a;
P = ((1-beta)*((1-beta)-Kb/Kr)*Kr+(beta*Kr*Kb/Kf))/a + 4*Mu/3;
b = N*beta*beta/K;
rho12 = rhoF*beta*(1-alpha);
rho11 = (1-beta)*rhoR-rho12;
rho22 = rhoF*beta-rho12;
ans = Q/Mu*((aA-bB+cC-dD)/(4*h*h)+(eE-2*fF+gG)/(h*h)) +
      R/Mu*((kK-lL+mM-nN)/(4*h*h)+(oO-2*pP+qQ)/(h*h)) -
      b*Fw*w*(hH-rR)/(2*delT*Mu) -
      rho22*(P-Mu)/(rho12*Mu)*((aA-bB+cC-dD)/(4*h*h)+(eE-2*fF+gG)/(h*h)) -
      rho22/rho12*(iI-4*fF+jJ+eE+gG)/(h*h) -
      rho22*Q/(rho12*Mu)*((kK-lL+mM-nN)/(4*h*h)+(oO-2*pP+qQ)/(h*h)) -
      rho22*b*Fw*w*(hH-rR)/(rho12*2*delT*Mu) -
      (hH-2*fF)*w*w*(rho12-((rho22*rho11)/rho12))/(delT*delT*Mu);
return ans;
}

```

```

float FHH(float aA,float bB,float cC,float dD,float eE,float fF,float gG,
          float hH,float iI,float jJ,float kK,float lL,float mM,float nN,
          float oO,float pP,float qQ,float rR)
{

```

```

a = (1-beta+(beta*Kr/Kf)-(Kb/Kr));
Q = (beta*(1-beta)*Kr-beta*Kb)/a;
R = beta*beta*Kr/a;
P = ((1-beta)*((1-beta)-Kb/Kr)*Kr+(beta*Kr*Kb/Kf))/a + 4*Mu/3;
b = N*beta*beta/K;
rho12 = rhof*beta*(1-alpha);
rho11 = (1-beta)*rhor-rho12;
rho22 = rhof*beta-rho12;
ans = Q/Mu*((aA-bB+cC-dD)/(4*h*h)+(eE-2*fF+gG)/(h*h)) +
      R/Mu*((kK-lL+mM-nN)/(4*h*h)+(oO-2*pP+qQ)/(h*h)) -
      b*Fw*w*(hH-rR)/(2*delT*Mu) -
      rho12*(P-Mu)/(rho11*Mu)*((aA-bB+cC-dD)/(4*h*h)+(eE-2*fF+gG)/(h*h)) -
      rho12/rho11*(iI-4*fF+jJ+eE+gG)/(h*h) -
      rho12*Q/(rho11*Mu)*((kK-lL+mM-nN)/(4*h*h)+(oO-2*pP+qQ)/(h*h)) -
      rho12*b*Fw*w*(hH-rR)/(rho11*2*delT*Mu) -
      (rR-2*pP)*w*w*(rho22-((rho12*rho12)/rho11))/(delT*delT*Mu);
return ans;
}

```

## LIST OF REFERENCES

1. Truver, Scott C., "Warfare Myth," *Proceedings*, pp. 36-43, October 1994.
2. Boutros-Ghali, Boutros, "The Land Mine Crisis," *Foreign Affairs*, pp. 8-13, September/October 1994.
3. BBN Systems and Technologies Report No. 7677, "Feasibility of Acoustic Land Mine Detection. Final Technical Report," May 19, 1992.
4. Stoll, R. D., *Sediment Acoustics, "Lecture Notes in Earth Sciences"*, Springer-Verlag New York, 1989.
5. Alterman, Z. S., Loewenthal, D., "Seismic Waves in a Quarter and Three Quarter Plane," *Geophysical Journal Royal Astronomical Society*, Vol 20, no. 2, pp. 101-126, 1970.
6. Chotiros, N.P., "Biot Model of Sound Propagation in Water-Saturated Sand," *The Journal of the Acoustical Society of America*, Vol. 97, no.1, pp. 199-214, 1995.
7. Deresiewicz, H., "The Effect of Boundaries on Wave Propagation in a Liquid-filled Porous Solid: IV. Surface waves in a Half-Space," *Bulletin of the Seismological Society of America*, Vol. 52, no.3, pp. 627-638. July 1962.
8. Ilan, A., Loewenthal D., "Instability of Finite Difference Schemes due to Boundary Conditions in Elastic Media," *Geophysical Prospecting*, no. 24, pp. 431-453, 1976.



## BIBLIOGRAPHY

Boyle F. A., Chotiros N. P., "Experimental Detection of a Slow Acoustic Wave in Sediment at Shallow Grazing Angles," Applied Research Laboratories - The University of Texas at Austin, 24 May 1991.

Kinsler, L. E., Frey A. R., Coppens A. B., Sanders J. V., *Fundamentals of Acoustics*, John Wiley & Sons, Inc. 1982.

Li, X., Zienkiewicz, O. C., Xie Y. M., "A Numerical Model for Immiscible Two-Phase Fluid Flow in a Porous Medium and Its Time domain Solution," *International Journal for Numerical Methods in Engineering*, Vol. 30, pp. 1195-1212, John Wiley & Sons, Ltd., 1990.

Sanyal, D.C., "On the Two-Dimensional Deformation of a Semi-Infinite Porous Elastic Medium," *Applied Science Research*, no. 26, pp. 227-245, 1972.

Smith, G. D., *Numerical Solution of Partial Differential Equations: Finite Difference Methods*, Oxford University Press, 1985.

Zhu, X., McMechan G.A., "Numerical Simulation of Seismic Responses of Poroelastic Reservoirs Using Biot Theory," *Geophysics*, Vol. 56, no. 3, pp. 328-329, 1991.



## INITIAL DISTRIBUTION LIST

1. Defense Technical Information Center.....2  
Cameron Station  
Alexandria, Virginia 22304-6145
  
2. Library, Code 52.....2  
Naval Postgraduate School  
Monterey, California 93943-5101
  
3. Department of Mathematics.....1  
Code MA  
Naval Postgraduate School  
Monterey, California 93943-5101
  
4. Department of Physics.....1  
Code PH  
Naval Postgraduate School  
Monterey, California 93943-5101
  
5. Clyde Scandrett.....1  
Code MA/Sd  
Naval Postgraduate School  
Monterey, California 93943-5101
  
6. Anthony A. Atchley.....1  
Code PH/Ay  
Naval Postgraduate School  
Monterey, California 93943-5101
  
7. Jonah W. Shen.....1  
4624 82nd Avenue Court West  
Tacoma, Washington 98466-2307
  
8. William F. Stewart.....1  
1095 Spruance Road  
Monterey, California 93940